METHANE CHEMISTRY

# Selective anaerobic oxidation of methane enables direct synthesis of methanol

Vitaly L. Sushkevich,[1]* Dennis Palagin,[1] Marco Ranocchiari,[1] Jeroen A. van Bokhoven[1,2]*

**Direct functionalization of methane in natural gas remains a key challenge. We present a direct stepwise method for converting methane into methanol with high selectivity (~97%) over a copper-containing zeolite, based on partial oxidation with water. The activation in helium at 673 kelvin (K), followed by consecutive catalyst exposures to 7 bars of methane and then water at 473 K, consistently produced 0.204 mole of $CH_3OH$ per mole of copper in zeolite. Isotopic labeling confirmed water as the source of oxygen to regenerate the zeolite active centers and renders methanol desorption energetically favorable. On the basis of in situ x-ray absorption spectroscopy, infrared spectroscopy, and density functional theory calculations, we propose a mechanism involving methane oxidation at $Cu^{II}$ oxide active centers, followed by $Cu^{I}$ reoxidation by water with concurrent formation of hydrogen.**

The high availability of methane as the principal component of natural gas, as well as its surge as a potent greenhouse gas (*1*, *2*), calls for the development of efficient methods for its conversion into commodity chemicals and liquid fuels (*3*–*7*). Specifically, direct conversion of methane into liquid chemicals suitable for transportation and storage still remains a major challenge (*8*). The current industrial route is indirect and relies on preliminary high-temperature and high-pressure oxidation to synthesis gas, a mixture of hydrogen and carbon monoxide, which can, in turn, react to form liquid methanol and hydrocarbons (*9*). This process, however, is only economically feasible at a very large scale and is not suitable for local, on-site applications, as, for instance, would be required to prevent flaring of the off-gas at remote oil-extraction facilities. Direct routes that have been explored (Fig. 1) range from homogeneous solution-phase processes (*10*–*12*) to heterogeneous chemical looping (*13*). However, no such system has found industrial application. A promising method that has received increasing attention is the stepwise conversion of methane to methanol over metal-containing zeolites (*14*–*19*) by using oxo-copper and -iron species as active sites, inspired by the natural biocatalytic enzyme systems (*20*–*22*). Nonetheless, neither synthetic catalysts nor chemical looping systems can yet convert methane directly into methanol at high yield and productivity (*23*). For instance, there is a need to find alternative routes that circumvent the difficulty of using a strong oxidant as a source of oxygen associated with the low methanol yield or the selectivity and costliness of oxidants (*24*).

We studied direct conversion of methane into methanol over the copper-exchanged mordenite zeolite (CuMOR), using water as the source of oxygen. We report here that water molecules not only act as a cheap and abundant source of oxygen to partially oxidize methane and regenerate the active sites but also facilitate desorption of the product, as well as stabilization of the reaction intermediates. The only product of the two-electron redox reaction with water is molecular hydrogen, which itself is a valuable species. With water acting as the oxidant, no molecular oxygen is needed. This effectively anaerobic oxidation allows an efficient low-temperature activation of methane, potentially suitable for local single-reactor conversion of the off-gas, and methane in general, into one of the main precursors for synthesis of chemicals.

The material for direct conversion of methane into methanol was prepared by a conventional ion-exchange procedure, with an aqueous copper nitrate solution and commercial sodium mordenite with a Si/Al molar ratio of 13. The as-prepared zeolite was dried and calcined in a flow of air at 773 K for 4 hours. The conversion of methane into methanol was studied in a multiple-cycle regime. The first cycle involved treatment of CuMOR at 673 K in a flow of either oxygen or helium, followed by cooling to 473 K and exposure to 7 bars of methane for 30 min, the conditions that increase the methanol yield (*18*) due to the higher activity of CuMOR observed at ramped methane pressure. Thereafter, water vapor in a flow of helium was introduced into the reactor, while the temperature was gradually increased to 673 K, which led to desorption of the products. After the complete desorption monitored by mass spectrometry (MS), the second reaction cycle was started by treatment of the zeolite with a flow of dry oxygen or helium (see detailed activation diagrams in fig. S1).

To directly compare the use of different oxidants, molecular oxygen was tested first. After the oxygen activation and a subsequent methane reaction, infrared spectroscopy detected methanol and methoxy species, as well as overoxidation products (carbon monoxide and formate species) on the surface of the CuMOR (fig. S2). The selectivity toward methanol observed in multiple cycles amounted to 85% for the oxygen-activated samples (figs. S3 and S4; details of the selectivity measurements are given in the Materials and Methods section of the supplementary materials). To increase the selectivity of the process, a softer oxidant was needed to avoid the formation of strong redox sites and to prevent the deep oxidation of methane. Because water may act as a soft oxidant (*25*), we investigated its efficiency for reactivation of CuMOR. In the first cycle, a fresh catalyst was activated under helium at 673 K, followed by methane reaction at 473 K, and methanol desorption upon water admission. A low selectivity of 87% and 0.142 mol $CH_3OH$ per mole Cu was detected (figs. S3 to S5). In the second cycle, after activation in He flow at 673 K, both selectivity and methanol yield increased substantially, suggesting that water is able to

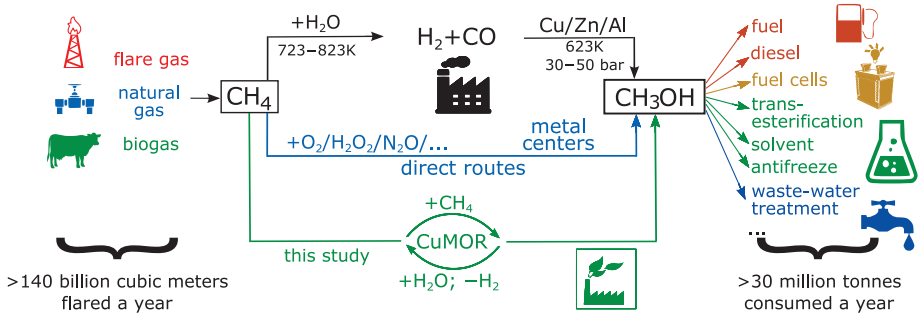


**Fig. 1. Current and proposed chemical processes for converting methane to methanol.** Although the route via synthesis gas requires harsh conditions and involves two separate steps, it is used to produce nearly 100% of methanol worldwide. Direct routes using oxygen, hydrogen peroxide, or other oxidants show promise with high selectivity and/or efficiency toward methanol. The approach proposed herein using water as an oxidant exhibits very high selectivity to methanol and requires neither harsh oxidants nor precious metal catalysts. Tonnes, metric tons.

[1]Laboratory for Catalysis and Sustainable Chemistry, Paul Scherrer Institut, 5232 Villigen, Switzerland. [2]Institute for Chemistry and Bioengineering, ETH Zurich, Vladimir-Prelog-Weg 1, 8093 Zürich, Switzerland.
*Corresponding author. Email: vitaly.sushkevich@psi.ch (V.L.S.); jeroen.vanbokhoven@chem.ethz.ch (J.A.v.B.)

regenerate the active sites (Fig. 2A). Both selectivity and yield of methanol remained constant over three additional cycles; the productivity stabilized at 0.202 mol $CH_3OH$ per mole Cu, and selectivity achieved 97%.

Reoxidation of the active sites and desorption of methanol from the CuMOR surface were induced by the presence of water vapor at 473 K and 1 bar total pressure. Introduction of water led to an increase of the mass spectral water signal, as well as the signal of the methanol desorbing from the zeolite (Fig. 2B). Additionally, the formation of hydrogen was observed before the appearance of methanol in the stream. This suggests the splitting of water, with the oxygen

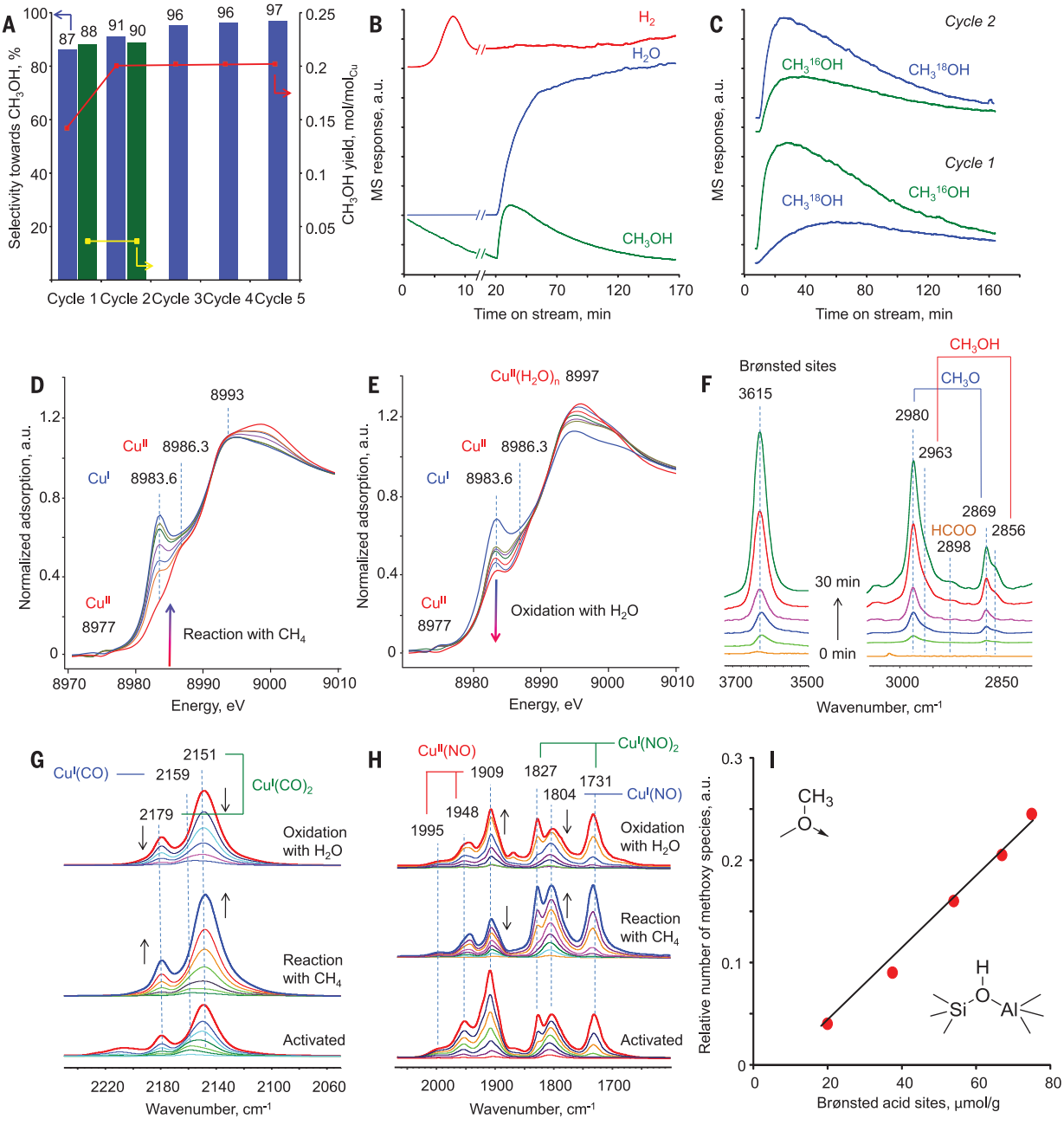


**Fig. 2. Experimental data.** (**A**) Methanol yield and selectivity across multiple cycles, each involving a helium activation at either 673 K (red line and blue bars) or 473 K (yellow line and green bars), followed by methane reaction and then catalyst reactivation by water at 473 K. (**B**) Mass spectral responses for hydrogen mass/charge ratio ($m/z$ = 2), water ($m/z$ = 18), and methanol ($m/z$ = 31) after the interaction with methane at 473 K and 7 bars, followed by a purge with water vapor in helium (2.6 vol%, 1 bar, total flow of 40 ml/min). (**C**) Mass spectral responses for unlabeled ($m/z$ = 31) and $^{18}O$-labeled ($m/z$ = 33) methanol after first and second reactivation with labeled $H_2{}^{18}O$, respectively. (**D**) In situ XANES spectra recorded during the interaction of CuMOR (pretreated in helium flow) with methane at 473 K. (**E**) In situ XANES spectra recorded during the interaction of water vapor with CuMOR at 473 K and 1 bar after the methane reaction. (**F**) Time-resolved in situ FTIR spectra of surface species formed during the interaction of CuMOR (pretreated in a flow of helium) with 7 bars of methane at 473 K. (**G**) FTIR spectra of CO adsorbed at 100 K onto CuMOR that was vacuum-activated (bottom), reacted with methane (middle), and reoxidized with water vapor (top). (**H**) FTIR spectra of NO adsorbed at 100 K onto CuMOR that was vacuum-activated (bottom), reacted with methane (middle), and reoxidized with water vapor (top). (**I**) Relative number of methoxy species versus number of Brønsted acid sites formed during the interaction of methane with CuMOR at 473 K within 5 to 120 min. a.u., Arbitrary units.

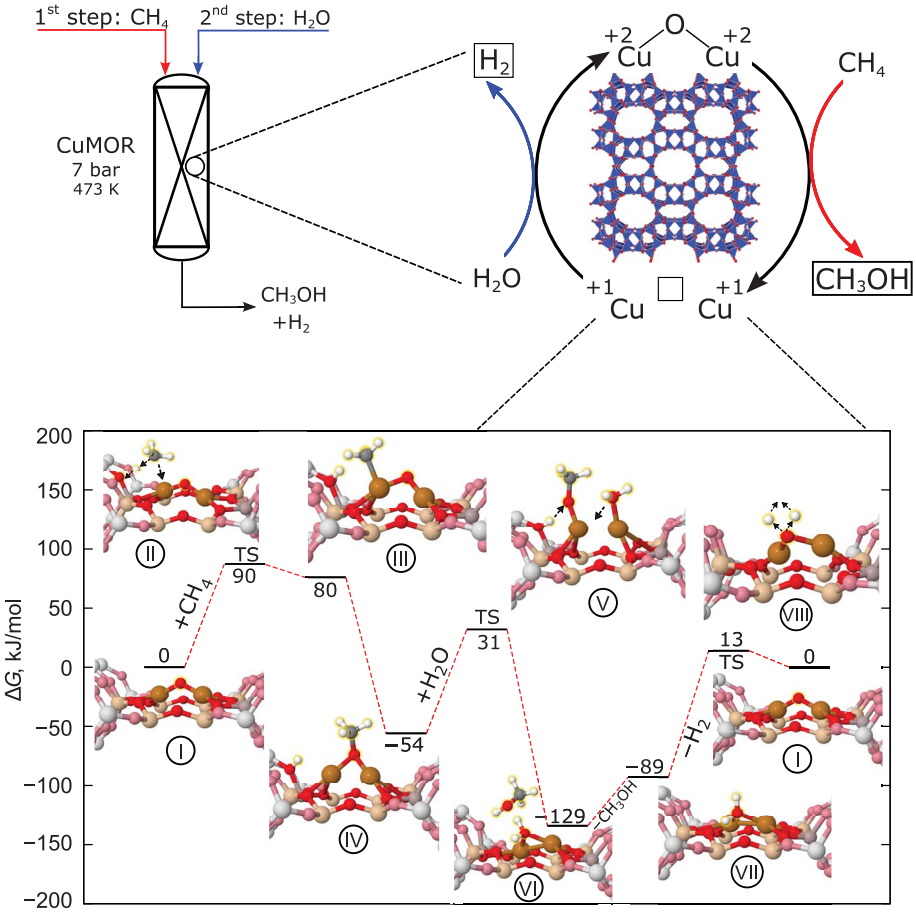


**Fig. 3. The mechanism of the partial oxidation of methane using water as oxidant.** (**Top**) Schematic representation of the reaction conditions of the partial oxidation of methane by water, involving the reduction of the dicopper site of mordenite and providing two electrons to stoichiometrically oxidize methane into methanol. Subsequent reduction of water into hydrogen returns two electrons for the rejuvenation of the mono(μ-oxo)dicopper active core. (**Bottom**) The DFT simulated pathway, illustrating the thermodynamic (Δ*G*, the change in Gibbs free energy) and kinetic feasibility of the proposed mechanism. Animated reaction pathway is available as movie S1.

atom used to reoxidize the copper sites and the hydrogen atoms assembled to form molecular hydrogen, which can easily desorb from the surface of the zeolite (fig. S6). The oxygen atoms become a part of the active center and react with a new methane molecule in the subsequent cycle (Fig. 2A). To confirm the insertion of oxygen atoms from water into the carbon-hydrogen bond of methane, we repeated the above experiments with $^{18}$O-labeled water, and compared the isotopic composition of methanol from both the unlabeled and $^{18}$O-labeled water-reactivated zeolite by MS (Fig. 2C and figs. S7 and S8). In the first cycle, mostly unlabeled methanol was formed, accompanied by the delayed release of $CH_3{}^{18}O$, indicating minor oxygen exchange on the surface of CuMOR. In contrast, after full desorption of methanol, followed by heating in helium at 673 K and a second interaction with methane, the MS signal from the labeled methanol increased considerably (Fig. 2C). Simultaneously, the signal from the unlabeled methanol decreased, pointing to the presence of $^{18}$O atoms in the active sites of CuMOR after interaction with water.

Such a redox process should be accompanied by a change in the copper oxidation state, which we monitored by in situ x-ray absorption spectroscopy (XAS) and Fourier transform infrared spectroscopy (FTIR) of adsorbed probe molecules; these methods have been successfully applied previously to study many redox materials, including copper-exchanged zeolites (*26*–*30*). The activation and reaction protocols were identical to those described for the reaction tests. The x-ray absorption near edge structure (XANES) spectrum of activated CuMOR showed a preedge feature at 8977 eV, characteristic of $Cu^{II}$, the absorption edge energy of 8993 eV, and a small shoulder at 8986.3 eV, which are indicative of a dominant copper oxidation state of $Cu^{II}$. A shoulder at 8983.6 eV indicates the presence of a minor fraction of $Cu^{I}$. The formation of $Cu^{I}$ atoms during the activation of CuMOR in helium is due to the autoreduction process, which is commonly observed for copper-exchanged zeolites starting at 473 K (*31*). Depending on the reaction conditions, along with the formation of different side products, the autoreduction process can lead to the loss of catalyst activity, as it causes the transformation of $Cu^{II}$ species into $Cu^{I}$ that are not active in methane oxidation.

Upon interaction with methane, the intensity of the peak due to $Cu^{I}$ species increased; this confirmed the reduction of copper by methane that led to the formation of oxidation products (Fig. 2D). Simultaneously, the oxygen atoms of the active sites reacted with methane, forming methanol or other oxidation products. Linear combination fitting (LCF) showed a decrease in the number of $Cu^{II}$ species (up to 70% of $Cu^{II}$ is converted into $Cu^{I}$) (see fig. S9). The interaction with methane, therefore, leads to the reduction of $Cu^{II}$ sites into $Cu^{I}$. To determine the oxidation state of copper during the interaction with water, the latter was introduced into the reaction cell and time-resolved x-ray absorption spectra were acquired. The XANES data showed that as soon as water was introduced, the intensity of the peak at 8983.6 eV decreased, indicating the oxidation of $Cu^{I}$. Simultaneously, the peak at 8997 eV due to the hydrated $Cu^{II}$ species appeared in the spectrum; this confirmed that water oxidized $Cu^{I}$ sites into $Cu^{II}$ (30% of $Cu^{I}$ was oxidized into $Cu^{II}$) (Fig. 2E and fig. S9). After 2 hours, 40% of $Cu^{I}$ sites were not fully reoxidized by water (Fig. 2E), which indicates that not all copper sites are reactive toward water. This could be due to coexisting different types of copper active species that have been identified in CuMOR (*32*).

To differentiate between various copper sites, FTIR spectroscopy of adsorbed carbon monoxide and nitric oxide, the most common probe molecules for studying $Cu^{I}$ and $Cu^{II}$ species (*26*, *27*), was used (Fig. 2, G and H, for CO and NO, respectively). Before each measurement, the CuMOR sample was preheated in vacuum at 673 K for 2 hours. At low CO coverages (pressure < 0.01 torr), the exclusive formation of $Cu^{I}$ monocarbonyl surface species was observed (2159 $cm^{-1}$). Increasing the carbon monoxide pressure led to the appearance of new bands because of the low- (2151 $cm^{-1}$) and high- (2179 $cm^{-1}$) frequency vibrations of $Cu^{I}(CO)_2$ dicarbonyl species (Fig. 2G). As was observed by XAS, the presence of $Cu^{I}$ in the activated samples relates to autoreduction. After the interaction with methane, the intensity of both bands increased due to the formation of additional $Cu^{I}$ sites. The positions of all three bands did not shift, indicating that the nature of copper sites interacting with methane and those undergoing autoreduction is similar. As expected, the subsequent interaction of the sample with water led to the partial reoxidation of $Cu^{I}$ sites, observed by the decrease of the bands at 2150–2180 $cm^{-1}$.

As the FTIR of the adsorbed carbon monoxide does not allow monitoring of the transformation of $Cu^{II}$ species, NO was used to access the changes in copper oxidation state. The data obtained after NO adsorption on the CuMOR sample activated in vacuum show the presence of bands at 1804, 1731, and 1827 $cm^{-1}$ that are associated with NO bound

to $Cu^{I}$ sites, as well as 1909, 1948, and 1995 $cm^{-1}$ assigned to different $Cu^{II}$ species (*26*, *27*) (Fig. 2H). After subsequent interaction of the freshly vacuum-activated CuMOR with methane at 473 K, the spectra of adsorbed NO showed an increase in the concentration of $Cu^{I}$ sites, accompanied by a simultaneous decrease in the quantity of $Cu^{II}$ sites, in line with both the FTIR spectra of the adsorbed carbon monoxide and XAS. After the vacuum-activated CuMOR sample reacted with methane, and subsequently with water, low-temperature adsorption of NO revealed a decrease of the bands associated with $Cu^{I}$ and an increase of the bands associated with $Cu^{II}$. In agreement with the XAS data, reoxidation with water did not induce full conversion of $Cu^{I}$ into $Cu^{II}$. Thus, only a fraction of copper sites that can activate the C–H bond of methane can be reoxidized with water; the rest of sites are not active. This explains the nonstoichiometric oxidation of methane with CuMOR, leading to a lower yield of methanol compared with the theoretical maximum [0.202 mol $CH_3OH$ per mole Cu versus 0.5 mol $CH_3OH$ per mole Cu].

The above results describe the processes that occur at the active sites of CuMOR without addressing the transformation of methane. To study the initial stages of methane activation over CuMOR, we applied time-resolved in situ FTIR spectroscopy. As we discussed above, the reaction of the helium-activated CuMOR with methane led to the formation of different surface species, including molecular methanol and methoxy groups (fig. S6). At the same time, a band at 3615 $cm^{-1}$ appeared, which is typical of Brønsted acid sites of the H–MOR zeolite (Fig. 2F). The number of observed Brønsted acid sites estimated from the FTIR spectroscopy of adsorbed pyridine scaled linearly with the total number of methoxy surface species (Fig. 2I). This indicates that the C–H bond cleavage coincides with methoxy and Brønsted acid site formation. The capacity of water to reactivate the oxidation sites of CuMOR suggests the possibility of partial methane oxidation without the need for temperature cycling. To test this, we carried out two cycles in which the CuMOR activation in a flow of helium, the reaction with methane, and the water reoxidation all occurred at 473 K without high-temperature treatment (Fig. 2A and fig. S10). In situ FTIR and MS confirmed the formation of methoxy species and methanol over the fresh CuMOR, as well as reoxidation of the material with water in the second cycle, indicating the feasibility of isothermal conversion of methane into methanol. However, the yield of methanol obtained for 473 K activation was much lower [0.04 mol $CH_3OH$ per mole Cu] than the yield from high temperature–activated CuMOR. This is caused by the poisoning effect of water, which was not desorbed at 473 K (*28*, *33*). It has been shown that a higher methane pressure has to be applied in the isothermal regime to compensate for the loss of activity (*18*). Following this protocol, we were able to partially recover the zeolite activity, which amounted to 0.08 mol $CH_3OH$ per mole Cu at 25 bars of methane.

The unique behavior of CuMOR relates to the reactivity of zeolite-supported copper oxide species. Overwhelming evidence in the literature suggests that there is no unique species that is solely responsible for zeolite activity; rather, a multitude of copper oxide clusters, such as monomeric, dimeric, and multimeric copper species, have been suggested as reactive toward methane in various zeolites (*14*, *15*, *17*, *18*, *34*, *35*). However, the limited size of the pores in mordenite stabilizes dicopper sites with bridged oxygen that mimics active sites of enzymes (*15*). Suitably, such an active center provides two electrons to stoichiometrically oxidize methane into methanol. The reactive oxygen in the Cu–O–Cu core could react with methane, yielding methoxy and reducing $Cu^{II}$ into $Cu^{I}$. Instead of the common reoxidation with oxygen, we showed that water returns two electrons, yielding reactive $Cu^{II}$ in concert with hydrogen formation (Fig. 3, top). To explain the oxidative behavior of water and to obtain detailed insight into the reaction mechanism, we studied the feasibility of such a process by density functional theory (DFT). We initially focused on the above described mono(μ-oxo)dicopper site (*15*), which supports the two-electron process and has the correct stoichiometry for typical ion-exchanged zeolite systems (*31*).

The calculated reaction profile is shown in (Fig. 3, bottom). Mono(μ-oxo)dicopper reacts with methane via the formation of a $CH_3$ fragment bound to a copper atom of the CuMOR active site and proton abstraction by the zeolite framework, which lead to the formation of a new Brønsted site (structure III, as seen experimentally in Fig. 2F). The calculated activation barrier amounts to 90 kJ/mol (structure II), which is comparable to the previously reported values corresponding to the classical methane "rebound" (*36*) mechanism (which, for our system, was also considered in figs. S11 and S12). After the activation of methane on the copper atom, a methoxy species is formed (structure IV) and both copper centers are reduced to $Cu^{I}$ (Fig. 2, D, G, and H). The formation of the methoxy species and the Brønsted site is exothermic by 54 kJ/mol. A subsequent direct desorption of methanol would produce a very high-energy $Cu^{+}\square Cu^{+}$ fragment (see fig. S11, structure $V^{B}$), which is unlikely to occur.

The addition of water relaxes the system via a relatively low-energy transition state ($\Delta E^{\neq}$ = 85 kJ/mol; structure V), that facilitates the reaction of the Brønsted site with the methoxy species to produce methanol and $Cu^{I}$–$OH_2$–$Cu^{I}$, stabilized by the formation of three additional hydrogen bonds (structure VI). Subsequent desorption of methanol (structure VII) is followed by the two-electron reduction process, which leads to the formation of molecular hydrogen (structure VIII, as seen experimentally in Fig. 2B), and, thus, regeneration of the original $Cu^{II}$–O–$Cu^{II}$ active site (structure I). The activation energy of the reduction process is calculated to be 102 kJ/mol, comparable to the methane-activation barrier, and thus makes such a process thermodynamically and kinetically feasible. The role of water is, therefore, twofold. First, it regenerates the catalyst by providing an oxygen atom for the two-electron reoxidation of the copper active center. The unique configuration of the mono(μ-oxo)dicopper active site enables water to act as an oxidant. Second, the presence of water ensures energetically favorable desorption of methanol. An excess of water molecules provides additional stabilization of the reaction intermediates and the transition states (see figs. S13 and S14), making the proposed mechanism more feasible. A survey of the literature shows that multiple copper species may be present and active toward methane activation (*14*, *15*, *17*, *18*, *34*, *35*). Further DFT calculations (see fig. S15) on copper trimer revealed that a similar mechanism of $Cu^{II}$ reduction by methane and subsequent reoxidation and hydrogen formation with water is equally likely for other species containing multiple copper atoms.

The anaerobic direct oxidation of methane to methanol demonstrated here is promising for cost- and energy-efficient, local on-site applications. After necessary further refinement of the herein proposed process to meet industrial requirements, the use of water instead of oxygen may contribute to development of an industrial process for the direct methane to methanol conversion.

## REFERENCES AND NOTES


1. E. G. Nisbet, E. J. Dlugokencky, P. Bousquet, *Science* **343**, 493–495 (2014).
2. D. Malakoff, *Science* **344**, 1464–1467 (2014).
3. C. Hammond, S. Conrad, I. Hermans, *ChemSusChem* **5**, 1668–1686 (2012).
4. B. G. Hashiguchi *et al.*, *Science* **343**, 1232–1237 (2014).
5. X. Guo *et al.*, *Science* **344**, 616–619 (2014).
6. S. H. Morejudo *et al.*, *Science* **344**, 563–566 (2014).
7. R. Schlögl, *Angew. Chem. Int. Ed.* **54**, 3465–3520 (2015).
8. A. I. Olivos-Suarez *et al.*, *ACS Catal.* **6**, 2965–2981 (2016).
9. K. Aasberg-Petersen *et al.*, *J. Nat. Gas Sci. Eng.* **3**, 423–459 (2011).
10. A. E. Shilov, *Pure Appl. Chem.* **50**, 725–733 (1978).
11. R. A. Periana *et al.*, *Science* **259**, 340–343 (1993).
12. R. A. Periana *et al.*, *Science* **280**, 560–564 (1998).
13. R. Palkovits, M. Antonietti, P. Kuhn, A. Thomas, F. Schüth, *Angew. Chem. Int. Ed.* **48**, 6909–6912 (2009).
14. M. H. Groothaert, P. J. Smeets, B. F. Sels, P. A. Jacobs, R. A. Schoonheydt, *J. Am. Chem. Soc.* **127**, 1394–1395 (2005).
15. J. S. Woertink *et al.*, *Proc. Natl. Acad. Sci. U.S.A.* **106**, 18908–18913 (2009).
16. E. M. Alayon, M. Nachtegaal, M. Ranocchiari, J. A. van Bokhoven, *Chem. Commun.* **48**, 404–406 (2012).
17. S. Grundner *et al.*, *Nat. Commun.* **6**, 7546 (2015).
18. P. Tomkins *et al.*, *Angew. Chem. Int. Ed.* **55**, 5467–5471 (2016).
19. B. E. R. Snyder *et al.*, *Nature* **536**, 317–321 (2016).
20. A. C. Rosenzweig, *Biochem. Soc. Trans.* **36**, 1134–1137 (2008).
21. S. I. Chan, S. S.-F. Yu, *Acc. Chem. Res.* **41**, 969–979 (2008).
22. L. Que Jr., W. B. Tolman, *Nature* **455**, 333–340 (2008).
23. M. Ahlquist, R. J. Nielsen, R. A. Periana, W. A. Goddard 3rd, *J. Am. Chem. Soc.* **131**, 17110–17115 (2009).
24. H. Schwarz, *Angew. Chem. Int. Ed.* **50**, 10096–10115 (2011).
25. T. Mitsudome *et al.*, *Angew. Chem. Int. Ed.* **47**, 7938–7940 (2008).
26. F. Giordanino *et al.*, *Dalton Trans.* **42**, 12741–12761 (2013).
27. E. Borfecchia *et al.*, *Chem. Sci.* **6**, 548–563 (2015).
28. E. M. C. Alayon, M. Nachtegaal, A. Bodi, J. A. van Bokhoven, *ACS Catal.* **4**, 16–22 (2014).

29. E. M. C. Alayon, M. Nachtegaal, A. Bodi, M. Ranocchiari, J. A. van Bokhoven, *Phys. Chem. Chem. Phys.* **17**, 7681–7693 (2015).
30. J. A. van Bokhoven, C. Lamberti, Eds., *X-ray Absorption and X-ray Emission Spectroscopy: Theory and Applications* (Wiley, 2016).
31. B. L. Trout, A. K. Chakraborty, A. T. Bell, *J. Phys. Chem.* **100**, 4173–4179 (1996).
32. P. Vanelderen *et al*., *J. Am. Chem. Soc.* **137**, 6383–6392 (2015).
33. P. Smeets *et al*., *J. Catal.* **256**, 183–191 (2008).
34. D. Palagin, A. J. Knorpp, A. B. Pinar, M. Ranocchiari, J. A. van Bokhoven, *Nanoscale* **9**, 1144–1153 (2017).
35. P. Tomkins, M. Ranocchiari, J. A. van Bokhoven, *Acc. Chem. Res.* **50**, 418–425 (2017).
36. G. Li *et al*., *J. Catal.* **338**, 305–312 (2016).

## ACKNOWLEDGMENTS

The authors acknowledge the use of the computing facilities of the Swiss National Supercomputer Center and are grateful for the Swiss Light Source and SuperXAS beamline for providing beamtime for XAS measurements. We thank the Energy System Integration platform of the Paul Scherrer Institute for financial support. Experimental data are available in supplementary materials. All authors are inventors on a patent application submitted by the Paul Scherrer Institut that covers the process described in the manuscript.

## SUPPLEMENTARY MATERIALS

www.sciencemag.org/content/356/6337/523/suppl/DC1
Materials and Methods
Figs. S1 to S16
References (*37*–*44*)
Movie S1

2 February 2017; accepted 13 April 2017
10.1126/science.aam9035

Editor's Summary

**A watery route from methane to methanol**

Methanol production is an expensive, energy-intensive process that initially overoxidizes methane to carbon monoxide. Sushkevich *et al.* used copper sites in a zeolite to oxidize methane to methoxy intermediates; they then added water to release methanol and hydrogen while reoxidizing the copper. This inexpensive process could prove useful at gas well sites for producing an easily stored and transported liquid from excess gas that at present is burned away.

*Science*, this issue p. 523